Title: Wear Resistant Solid Lubricating Coatings via Compression Molding and Thermal Spraying Technologies

Authors: Samantha Michelle Gateman,[a†] Sima Ahmad Alidokht,[b] Emmanuel Mena-Morcillo,[a] Robert Schulz,[c] Richard R. Chromik,[b] Anne-Marie Kietzig,[d] Ivan P. Parkin,[e] Janine Mauzeroll[a*]

Corresponding Author

*e-mail: Janine.mauzeroll@mcgill.ca, phone: +1-514-398-3898

Affiliations

[a]Laboratory for Electrochemical Reactive Imaging and Detection of Biological Systems, McGill University, Montreal, QC H3A 0B8, Canada

[b]Department of Mining and Materials Engineering, McGill University, Montreal, QC, H3A 0C5, Canada

[c]Institut de recherche d'Hydro-Québec, Varennes, J3X 1S1, Canada

[d]Department of Chemical Engineering, McGill University, Montreal, QC, H3A 0C5, Canada

[e]Materials Chemistry Department, University College London, London, WC1E 6BT, United Kingdom

KEYWORDS: Thermal spray coatings, polymer coatings, wear resistant, solid-lubricating, compression molding

ABSTRACT

This work combines two industrially friendly processing methods in order to create wear resistant and solid-lubricating composite coatings potentially suitable for high load applications. Layered composite coatings were fabricated over wrought stainless steel 444 (SS444) by compression molding a mixture of solid lubricant polymer, polytetrafluoroethylene (PTFE, 80 wt%), and wear resistant polymer, polyimide (PI, 20 wt%), onto iron aluminide (Fe_3Al) thermal spray coatings without the need of either primers or adhesives. The fabrication process consisted of three main steps: deposition of the Fe_3Al thermal spray coating onto a SS444 substrate and transfer into a metal mold; transfer, compress, and sinter mixed polymeric powder onto the thermal spray coating; and finally, sample cooling to room temperature. This method takes advantage of the high surface roughness of thermal spray coatings, which increases mechanical adhesion of slippery PTFE to the underlying metallic material. Coatings were produced with and without a small amount of graphite (5 wt%) to analyze its impact on sliding and wear properties. Unlike current coating technologies, the thickness of the coatings presented herein can be easily and quickly tailored by varying the amount of polymer powder added to the mold prior to compression, or by grinding after fabrication. We produced and analyzed coatings ~1.3 mm in total thickness that portray coefficient of frictions ~0.1, similar to that of pure PTFE. The calculated wear rates for both coatings with and without graphite are an order of magnitude lower than what has been previously reported for coatings of similar composition. The influence

of graphite on wear properties was found to be minimal due to the high content of self-lubricating PTFE, yet can act as a way to lower material costs and increase the coatings load capacity.

1 INTRODUCTION

In many industrial sectors such as oil, gas, and hydroelectric, sliding or rolling contacts are common in machine parts, where low friction and high wear resistance are needed to increase efficiency and service life of the infrastructure.[1] Solid lubricating materials have become a popular alternative to liquid lubricants and grease due to their ability to reduce maintenance costs and environmental impact. Solid lubricants also play a vital role in applications that do not permit the use of external lubrication such as in aerospace, food industries and medical treatment products.

Polytetrafluoroethylene (PTFE), or Teflon®, is the most commonly used solid lubricant because of its resistance to chemical attack, high melting point, and biocompatibility.[2,3] Its low dry sliding friction coefficient ($\mu < 0.2$) on a variety of counterface materials is attributed to the low shear strength of the long (CF_2-CF_2) chains[4] and the transfer of polymeric material to the counter surface, creating a well-adhered thin transfer layer that results in the sliding of two soft polymeric surfaces.[5,6]

Despite its excellent sliding properties, PTFE suffers from poor wear resistance and excessive viscoelastic deformation under load,[7] which greatly limits its use in high load bearing applications. The incorporation of almost any type of reinforcing fillers into PTFE including inorganic (metals, metal oxides/carbides)[4,8,9] and organic (carbon fiber, graphite, polymer blends)[10–13] materials has been shown to reduce wear and increase load capacity. In cases where metal fillers are utilized, there are often corrosion issues such as galvanic corrosion with the counter metal that limit their applications. Furthermore, purely polymeric composite systems still portray relatively low load capacities with low pressure-velocity limit values.[14] Therefore, this work strives to develop a new wear resistant solid-lubricating layered composite coating system that is functional at high loads by combining industrially relevant technologies: thermal spraying and compression molding.

Thermal spray methods are responsible for the success and safety of many renewable/non-renewable energy divisions and industrial sectors including biomedical, automotive, and aerospace due to their strong mechanical adhesion to substrates and ability to form dense, wear resistant coatings.[15] Consequently, the implementation of thermal spray technology to create high load bearing and wear resistant solid-lubricating coatings has been previously documented.[16–19] Two approaches have been reported: multilayered coatings and mixture composite systems. The layering approach uses thermally sprayed inorganic coatings as the bottom layer with a PTFE-based topcoat to utilize the tribological and chemical abilities of the two layers, respectively.[16,17] PTFE coatings have been previously applied using air spraying[16] and physical vapour deposition.[17] However, due to the poor adhesion of the solid

lubricant with the metal substrate, the use of a primer layer (i.e., polymer binders) was required to increase adhesion and inhibit delamination. This poses another step in the fabrication process, increasing both processing time and cost, as well as having a negative environmental impact.

The mixture composite approach combines both the inorganic material with the polymer to create composite coatings.[18,19] Yamane *et al* fabricated binary metallic thermal spray coatings with arranged PTFE reservoirs designed to support the load on both the hard metallic thermal spray coating and the slippery PTFE sections.[18] Although wear rates decreased, the coefficient of friction of the composite coatings were inferior to pure PTFE and such coatings remain vulnerable to chemical degradation. Another study conducted by Mateus *et al* consisted of co-spraying ceramic and PTFE powders to create composite coatings via thermal spraying.[19] PTFE thermal spray coatings build up is difficult due to its low adherence and high viscosity while in a molten state, which results in issues during splat formation.[19] Furthermore, thermal spraying polymeric material is tricky due to their low melting temperatures and irregular particle morphology/size that can cause clogging of the spray nozzle. While the researchers were able to co-deposit PTFE and ceramic material using ideal injection systems to form composite coatings, the coatings portrayed poor scratch resistance and low adhesion between the ceramic and PTFE. As a result, a thermal post-treatment was required to increase adhesion. Despite such efforts, the coefficients of frictions reported were much higher than pure PTFE (0.4 at steady state).

Alternatively, the work presented herein implements hard metal thermal spray coatings as a bottom layer under a PTFE-based polymeric film formed via compression molding of polymer powder. This methodology minimizes corrosion, the coefficient of friction, and processing time;

by fabricating a solid-lubricating, layered coating structure capable of withstanding high loads and wear without further post modifications.

Compression molding is one of the most common methods to produce freestanding PTFE[20–22] and PTFE composite objects.[4,9,23] The process involves transferring polymeric powder into a mold of desired shape/dimensions, followed by applying heat and pressure for a period of time before cooling back to room temperature. This method is attractive due to its ability to make complex geometric shapes, produce excellent surface finishing, and due to its reliability on large quantity manufacturing.[24] Although a popular method for fabricating freestanding material, there lacks an effort to apply compression molding to form PTFE-based coatings onto metallic substrates. Current methodologies to create PTFE coatings include physical vapor deposition,[17,25] electroplating,[26] air[16,27] and thermal[19] spraying, immersion deposition,[18,28] and spin coating.[29] The resulting coatings typically require a post heat treatment to encourage densification and adhesion. Additionally, thicknesses range from 1-50 μm, which are thin enough to be easily perforated during erosional processes.[17] By utilizing compression molding, we are able to fabricate much thicker polymer coatings to increase the lifespan of the material, without post modifications. The high surface roughness of as sprayed thermal spray coatings (S_a ~12μm)[30,31] increases the mechanical adhesion between the polymer and metal layers to avoid the use of adhesive additives/layers. Another advantage of combining these to coating methods is that both can be applied to curved surfaces, where geometrically complex parts can be easily coated for protection. A high wear resistant and thermally stable polymer, polyimide (PI), is added to the PTFE matrix as a filler in order to further reduce wear and possibly encourage chemical adhesion to the metal thermal spray bottom

layer.[32–34] Coatings with and without a solid lubricating graphite additive are fabricated and their tribological properties are compared.[35]

2 MATERIALS AND METHODS

2.1 Thermal Spray Coating Fabrication

The underlying thermal spray coatings were prepared using iron aluminide (Fe_3Al) (Ametek, Eighty Four, Pennsylvania, USA) water atomized powder. The irregular shape of water atomized particles increases the materials surface roughness, unlike spherical gas atomized particles, thus increasing mechanical adhesion of the polymeric material to that of the metal substrate. The metallic powder was ball milled using 3 mm diameter stainless steel balls (horizontal stainless steel mill CM08, ZoX Simoloyer Inc, Wenden, Germany) for 9 h and sieved to achieve a mean particle diameter of 25 ± 11 μm as measured by laser diffraction (HORIBA LA-900, California, USA).

The thermal spray coatings were fabricated using a high velocity oxygen fuel (HVOF) spraying torch (JP-8000 Praxair) with 4" nozzle length and liquid kerosene as the fuel source. The substrates were 6 × 10" plates of wrought stainless steel (SS) 444 produced by ArcelorMittal, sandblasted prior to HVOF spraying via alumina grit blasting (270 μm) to induce a surface roughness (R_a) of 2.1 μm. Spray parameters include a powder feed rate of 44 g/min, stand-off distance of 13", and 15 passes were used to create ~300 μm thick coatings. The oxygen and kerosene fuel flow rates were 732 L/min and 28 L/h, respectively, using a combustion pressure of 655 kPa. The argon flow rate was 4.5 L/min. The coating was then section into circular coupons 16 mm in diameter via water jet cutting for further analysis and polymer coating application.

2.2 Mold Fabrication

A steel mold was fabricated to fit the 16 mm diameter circular HVOF coupons. The mold was made of tool steel, where the raw material was pre-machined before heat treatment for hardening. In order to achieve a slide fit, the mold parts were then ground to precise dimensions. A schematic and images of the mold can be found in Figure 1.

2.3 Compression Molding of Polymeric Composite Coatings

Two, pre-mixed polymeric composite powders were donated (Ensinger HP Polymer GmbH, Lenzing, Austria). The first composite powder had a composition of 20% PI and 80% PTFE and was dark yellow in colour, while the other consisted of 20% PI, 75% PTFE, 5% graphite, giving it a light gray colouring.

HVOF coated coupons were transferred into the bottom of the mold, on top of the bottom pin that avoids direct contact with the hot plates. About 0.3 g of polymeric powder was added and spread evenly onto the HVOF surface within the mold using a spatula. The pressure pin was loaded into the mold to seal the HVOF coupon and polymer powder inside, and the entire system was transferred into the compression press. The system was heated to a temperature of 330 °C while under 5000 psi of pressure for 30 min, as suggested by the polymer powder suppliers for compression molding of free-standing objects. This is around the melting temperature of PTFE (326 °C)[36] and slightly higher than the glass transition temperature of PI (315 °C),[37] insuring flowability and hence maximizing adhesion between the two polymeric materials as

well as with the metal HVOF coated substrates. The system was then removed from the compression press and left to cool down for 30 min before removing the sample.

It is important to mention that coatings were also attempted over both mirror polished and sandblasted SS 444, however, due to the lack of surface roughness, there was not enough mechanical adhesion at the polymer-metal interface and delamination occurred.

2.4 Thermal Gravimetric Analysis (TGA)

The thermal stability of the polymeric powders was studied (Discovery TGA 5500, TA Instruments). About 9-10 mg of sample was transferred into weighing trays and the temperature was ramped from room temperature to 1000 °C at a rate of 20 °C min^{-1}. The experiments were carried out under air with a flow rate of 20 mL/min.

2.5 Microscopy and Chemical Analysis

Scanning electron microscopy (SEM) (SU 3500 variable pressure, Hitachi) equipped with energy-dispersive X-ray spectroscopy (EDX) (Oxford, Inca, Silicon drift detector) for elemental composition determination was used to image the cross section of the layered coatings. The electron microscope was utilized under 30 Pa of pressure and incident beam energy of 15 kV. Prior to imaging, all cross sections of samples were ground using 800-4000 grit SiC pads and polished to a final step using 0.05 μm Alumina slurry.

All confocal microscopy data for surface roughness analysis and wear track profiles was recorded using a white light interferometry profiler (NewView, Zygo) and Mx™ software.

Chemical analysis of the polymeric films, HVOF coatings, and interface was carried out using an Al K-Alpha X-ray photoelectron spectrometer (XPS) (ThermoFisher). Prior to analysis, surfaces were sputtered clean with 1000 eV Ar^+ ions. The spot size was 200 μm and 10 scans were performed per spectrum. Each region was analyzed 3 times to insure reproducibility.

2.6 Tribological Testing

Sliding wear measurements were performed in air (30-35% relative humidity) using a custom-built ball on flat reciprocating tribometer. Counterfaces used were spheres of AISI stainless steel 440C with a diameter of 6.5 mm. All testing was conducted with a normal load of 10.7 N, sliding speed of 10 mm/s, track length of 6 mm, and were run for 10,000 cycles (sliding distance of 120 m). A piezoelectric sensor mounted underneath the sample stage measured friction forces with a sampling rate of 800 Hz. The average coefficient of friction (COF) across the middle of the wear track was graphed versus the number of cycles. Sliding tests were repeated at least 4 times for each condition. The volume removed during wear testing, v (mm^3), was measured using a white light interferometry profiler, obtained by multiplying the profilometry-measured cross-sectional area of the material removed by the track length. Using the total sliding distance, x (m), and the applied load, W (N), the wear rate, k (mm^3/Nm) was calculated:

$$k = \frac{v}{Wx} \quad [1]$$

As previously used to estimate wear rate of coatings in previous studies.[38–40] All wear tests were done on as-casted coatings (no grinding/ polishing).

3 RESULTS AND DISCUSSION

3.1 Fe_3Al Thermal Spray Coatings

Fe_3Al is an excellent candidate material for implementation in high temperature environments due to its resistance to sulfidizing/oxidizing and low cost.[41] Research efforts have focused on the industrialization of Fe_3Al by using thermal spray methods in order to solve difficulties in shaping the material.[41–43] Electron microscopy images of the underlying Fe_3Al HVOF coatings surface can be found in Figure 2. The HVOF coatings are well adhered to the stainless steel substrate, where no delamination was observed. The surface of the coatings is rough (S_a ~13 μm via confocal microscopy) with a hierarchical sub-micron/micron textured surface (Figure 2B). The high surface roughness of the HVOF coatings enable maximum mechanical adhesion to the polymeric coating.

The chemical composition of the Fe_3Al HVOF coatings can be found in table 1. The main composition of the coatings is Fe and Al, while Cr and Si are added to improve mechanical properties. The presence of oxygen is due to the thermal oxidation of the material occurring in flight during the spraying process and during powder atomization. High amounts of carbon are also detected on the surface of the coatings, stemming from the deposition of residual carbon from the fuel source, kerosene,[30] and/or from the deposition of contaminating volatile organic compounds on the coating's surface.[44] This chemical analysis is in agreement with Fe_3Al HVOF coatings that have been previously reported.[45]

Although Fe_3Al HVOF coatings portray high adhesion and strength, low porosity, and high-temperature erosion resistance,[46] they show poor wear resistance at room temperature (k ~ 10^{-3} to 10^{-4} mm^3/Nm) and high COF (>0.8).[47,48] Hence, the addition of hard ceramic fillers

such as TiC,[48] TiB,[47] and WC[46] have been implemented to improve wear rates. Despite improvements in wear resistance, high COF render such coatings unsuitable for protecting moving parts in infrastructure. Thus, this work acts as a proof of concept to successfully compression press PTFE composite coatings onto pure Fe_3Al HVOF coatings to produce a layered, well-adhered, and solid lubricating coating with moderate wear rates and low COF.

3.2 Polymer Thermal Stability

The thermal stability of the composite polymeric powders was investigated using thermal gravimetric analysis under air to confirm the stability of the material during thermal compression molding. Typical TGA traces obtained from the powders with and without graphite addition are shown in Figure 3. The materials did not lose any significant mass until an offset point was reached at a temperature of 568 °C for the PTFE/PI material and 575 °C for the PTFE/PI/graphite material. The slight increase in offset temperature for the powder containing graphite is simply due to the presence of graphite. These values are in agreement with what has been reported previously for similar composite materials.[49] The degradation process continued until about 650 °C for the PTFE/PI powder when the weight % reached nearly zero, indicating the complete combustion of the sample. The powder containing graphite underwent another combustion process at 725 °C, which corresponds to the burning of graphite.[50,51] The PTFE/PI/Graphite powder was completely burnt at around 810 °C. This analysis confirms the thermal stability of the two materials during compression molding at 330 °C.

3.3 Coating Structure and Interface

Polymer coatings with and without graphite were compression press molded onto the flat HVOF thermal spray coatings using 0.3 g of polymeric powder. The cross sections of the resulting layered composite coatings can be found in Figure 4. Both polymeric layers, PTFE/PI (Figure 4A) and PTFE/PI/Graphite (Figure 4B), are about 1 mm in thickness.

The PI particles are darker in contrast due to the polymer's consisting elements having a lower atomic mass (i.e. Oxygen, Nitrogen) in comparison to PTFE (i.e. Fluorine), and are homogeneously distributed throughout the PTFE matrix as particles due to their high melting point. Neither voids/pores nor cracks are observed within the polymeric coating, presenting a dense and defect-free polymer top layer. The polymer layer is also in good contact with the HVOF coating, where no voids/pores are observed at the interface.

Magnified SEM images of the interface of the HVOF and polymeric coatings can be seen in Figure 4i and 4ii for coatings without and with graphite, respectively. EDX mapping shows the local elemental composition of the magnified cross-section image at the interface for elements of Fe, F, and C. The polymer layer is in direct contact to the HVOF metallic coating, where the PTFE matrix has penetrated the valleys and voids within the surface of the thermal spray coating for both types of polymeric films. PI particles can be observed as the regions within the polymer coating that is lacking F (as pointed out in Figure 4i/ii). It can also be seen that both PI and PTFE are in contact with the HVOF coating, indicating the possibility of bonding, and hence, chemical adhesion, between PI and metallic coatings that would increase the total adhesion between the two layers. This is further investigated in later sections.

Although we demonstrate this coating system on flat substrates, both thermal spray technology[52,53] and compression molding[54,55] can be applied to curved objects. The combination of the two methodologies presented here has potential to be an attractive fabrication process for coating real industrial parts with complex geometric shapes. Certain challenges for coating curved surfaces that would need to be addressed in future studies include designing and fabricating molds, the uniformity of the thermal spray coating at sharp or angular regions, and limitations of material flow within the mold cavity.

The surface of the polymeric composite films is shown in Figure 5A with corresponding surface roughness measurements obtained using an optical profilometer, as shown in Figure 5B. A total of 6 measurements were taken to result in an average surface roughness, S_a, of 0.4 ± 0.1 μm. The difference in height of the PI particles and the PTFE matrix could be due to the difference in compression strengths and/or of different thermal properties of the polymers as they cool. The low surface roughness encourages a lower coefficient of friction at initial stages of wear,[56] which is measured in the next section.

3.4 Tribological Testing

The sliding capabilities of the composite polymeric coatings were plotted in terms of coefficient of friction (COF) with respect to the number of cycles as seen for coatings without (Figure 6A) and with (Figure 6B) graphite. It can be seen for both coatings that the COF increases until reaching steady state. COF curve for PTFE/PI/Graphite reached steady state value of 0.1 at around 2000 cycles, whereas PTFE/PI displayed slightly higher steady state COF value

which was developed at longer sliding cycles. Similar values have been reported for unfilled PTFE in previous studies.[3,4]

The values measured in this work are compared to pure PTFE and PI as well as PTFE/PI composite materials in Table 2. The average COF of both coatings fabricated are lower than what has been previously reported for PTFE/PI composite materials of similar compositions. In the case of Su *et al*'s work,[34] this could be due to the higher content of PI, and/or the fabrication method chosen, a spraying technique, which produces coatings with a higher surface roughness and lower density in comparison to the coatings presented in this work. It should be noted, however, there are many parameters to take into consideration during sliding testing (counter material, sliding speed, normal load, experimental set up, relative humidity, etc.) that can result in different COF values.

To understand the coatings' wear and sliding behaviors, we studied the resulting wear tracks and corresponding counter spheres using SEM/EDX. Previously, the COF evolution of the top polymer coatings (run-in period and gradual increase) was accounted to the transfer film formation on the counter material.[33,34] The evaluation of the counter spheres was performed to observe the presence of a transfer film and/or wear of the balls. No wear was observed; indicating the contact pressure during testing was consistent. The formation of a transfer film could lead to circulation of third-bodies from the surface's interface to the counter spheres and back onto the polymer surface. The morphology, structure, and adhesion of transfer films to the counter sphere have all been found to be strong predictors of friction and wear properties. From the SEM images in Figure 7, no bulk transfer film was identified that resulted from wear testing

of both thick coating systems. However, there are small patches of thin local transfer films observed on the counter spheres, in contact regions, as well as wear debris. The EDX point chemical analysis of such debris and thin polymer transfer films can be found in Table 7. All material found on the counter spheres mating with PI/PTFE are rich in PTFE, which provides evidence of PTFE displacement and therefore PI enrichment within the wear tracks. Whereas local transfer films identified on counter spheres sliding on PI/PTFE/graphite was rich in carbon, implying graphitic transfer film formation.

Images of the wear tracks for both coating systems can be found in Figure 8. Materials are scraped from the contact area as seen at the edges of the wear track. Chemical analysis of extruded chips on the side of wear tracks showed that this material was mostly PTFE. Inside the wear tracks, a high density of PI particles can be seen in comparison to outside the wear tracks. EDX point analysis inside and outside the wear tracks confirmed this enrichment of PI inside the wear tracks, where more F was found outside and a higher content of N and O were detected inside, as presented in Table 4. The enrichment of PI inside the wear tracks is therefore responsible for the gradual increase in COF during the run-in period, yet this enrichment does not increase the COF above a value greater than the COF of pure PTFE.

The coatings with 5 wt% graphite additive portrayed a smaller confidence interval for COF values in comparison to coatings without graphite, a trend that has been reported previously.[57] This may be caused by a slightly better locally adhered transfer film produced from coatings with graphite addition to the counterface,[58] and/or due to a simple relationship between friction and contact stress. The addition of graphite was also shown to decrease the percentage of

deformation under load by the polymer powder suppliers, Ensinger, and has been previously documented as a method to increase load capacity.[10] Thus, such coatings may bear a higher load capacity than coating without the graphite additive.

It has been shown in previous studies for PI coatings without PTFE that the addition of graphite can significantly decrease the COF value of the system, where 25 wt% of graphite additive demonstrates a COF of 0.15.[59] However, we observe no change in value between the two coating systems studied here since PTFE is already an excellent solid lubricating agent. Regardless, we show that a 5 wt% of graphite does not negatively impact the COF, and therefore could also be a method for decreasing the cost associated with materials for coating production. This could be particularly important for coating large industrial infrastructure.

The wear rates of the coatings were also calculated and averaged. Both coatings exhibit wear rates two orders of magnitude lower than that of pure PTFE, indicating that the addition of PI increases wear resistance. The wear rate values obtained for each coating are not significantly different from one another, further validating the use of graphite to lower production costs. In comparison to similar studies presented in Table 2, the coatings developed here portray order of magnitude lower values for wear rates. This could be due to the density of the compressed coatings in comparison to the sprayed coatings,[34] and due to the influence of the underlying metallic HVOF thermal spray coating in comparison to the free standing PTFE/PI materials.[33]

After 10, 000 cycles, only about 50 μm of the coatings was penetrated. The thickness of the coatings presented are about ~1 mm, indicating a long lifespan of the material. This can be

controlled by adding more polymeric powder to the compression mold prior to compression molding, so it is possible to fabricate even thicker polymer coatings on top of the thermal spray substrates to further increase the coatings lifespan. Due to the thickness of the coatings produced in this work, the interface between the polymer and HVOF layers was not reached during tribological analysis. It was attempted to polish the coatings prior to wear testing in order to reach the polymer/metal interface and study the transition region during wear experiments. Perforation of the coatings during wear testing to expose the metallic HVOF coating was successful, as bright areas in back-scattered electron microscopy images (not shown) indicate a material with a high atomic mass and was confirmed using EDX point analysis. However, we still were unable to see such a transition region in the tribological measurements. The behavior of this interface, i.e., when the top polymer layer has been comprised and the exposure of the HVOF coating is present, will continue to be investigated in future studies.

Lastly, no delamination of the polymer coatings from the metal thermal spray substrates was detected after wear testing. This adhesion between the two coatings can be explained by the high surface roughness of the HVOF coatings, therefore increasing mechanical adhesion. There is also the possibility of chemical bonding, and hence chemical adhesion, occurring at the interface. The chemical composition of the polymer/metal interface is investigated in the next section in order to better understand the adhesion mechanism occurring.

3.5 Chemical Composition and Adhesion of Polymer/Metal Interface

In order to understand the adhesion mechanism of the polymer film to the HVOF metallic surface, the interfaces were investigated using XPS- one of the most utilized techniques for revealing changes in surface chemical states and hence chemical adhesion mechanisms.[60,61]

C 1s regions were analyzed for coatings with and without graphite as shown in Figure 9. Spectra were taken on the polymeric coating, HVOF coating, and interface for each coating and were fit to theoretical binding energies of present carbon species. It can be seen for both coatings that the HVOF coatings' surface contains carbon species including C=O, C-O, and C-C, which are present due to the deposition of kerosene and VOCs, as shown previously for SS HVOF coatings produced using the same parameters.[30] The carbon XPS spectra of the polymeric coatings shows the inclusion of PTFE and PI in the composite polymer film by the presence of $C\text{-}F_2$ at about 292.0 eV and C=O at 289.0 eV (from the imide functional group) binding energies, respectively.

The presence of carbon metal bonds has been previously detected on both PTFE[29] and PI.[62] Binding energies for Ti and Cr carbon bonds formed between sputtered metal and spin coated PTFE films was observed at 282.0 eV and 283.0 eV, respectively, which explained the increase in peel strength measured for such materials.[29] However, neither shifts nor satellite peaks to lower binding energies were observed in the spectra collected at the interface in this work, nulling the hypothesis that chemical adhesion between PTFE and the metal thermal spray coatings exits.

Atanasoska *et al* used XPS to study the formation of chemical bonds at an aluminum/PI interface via in-situ vapor deposition at room temperature and after sintering at 300 °C. At both temperatures, the formation of Al-O bonds was observed and attributed to a C-O-Al complex compound where annealing resulted in a less selective but higher reaction of Al with PI.[62] Such analysis is difficult for the system under investigation in this study since Al-O bonding is present in the Fe_3Al thermal spray coatings due to thermal oxidation during spraying. Yet, due to the literature regarding the presence of chemical bonding at the interface of metal/PI systems[62,63] as well as the excellent adhesion observed during tribological measurements, the formation and presence of chemical bonding between the PI and metallic coatings cannot be ruled out. Furthermore, we attempted to fabricate pure PTFE films on top of the HVOF coatings in a similar manner, but the resulting coatings did not portray good adhesion between the polymer and metal i.e. delamination occurred prior to any tribological testing, indicating the importance of PI on adhesion. Thus, further investigation is required to better understand such phenomenon and will be carried out in future works. Nonetheless, by utilizing high surface roughness HVOF coatings as a substrate for compression molding PTFE/PI composite coatings, adhesion is maintained after extensive tribological investigation. This method could be utilized as an alternative technique for adhering slippery PTFE composite coatings onto metallic surfaces instead of using more complex and expensive methods including ion beam and plasma sputtering, or direct chemical treatments.[64–67] Therefore, we are currently investigating the outcome of this coating method on various types of thermally sprayed materials.

4 CONCLUSIONS

Layered metal thermal spray and polymeric composite coatings have been fabricated to produce wear resistant and solid-lubricating materials by compression press molding. The high

surface roughness of the thermal spray coatings and presence of PI increases adhesion between the two coatings, minimizing the possibility of delamination. Two PTFE composite powders with and without graphite were implemented for coating fabrication and analyzed for their tribological properties. Both coatings portrayed low values of COF and relatively high wear resistance in comparison to what has been previously reported, although under slightly different conditions. The addition of 5 wt% graphite stabilized the coating's COF, but no significant difference in COF nor wear rate values were found, indicating that small substitutions of graphite for PTFE is an acceptable method of minimizing costs and can increase the coatings load capacity. This coating fabrication process is tailorable to produce any desirable polymeric film thickness and can be utilized for making thick (> 1mm) solid lubricating coatings without the need of adhesives or non-industrially friendly adhesion methods.

5 AUTHOR INFORMATION

Present Addresses

† Sorbonne Université, CNRS, Laboratoire de Réactivité de Surface UMR 7191, 4 Place Jussieu, 75005 Paris, France

Author Contributions

S.M.G. conceptualized, designed, and fabricated the layered polymeric-metal coatings, analyzed SEM cross-section images, and was the major contributor to the data analysis and manuscript preparation. S.A.A. performed wear tests and SEM analysis of wear tracks and counterfaces. E.M.M. reproduced coating fabrication and performed XPS measurements. All

authors provided discussion and contributed to proof reading. All authors have given approval to the final version of the manuscript.

Funding Sources

The work presented was financially supported NSERC CRD 242399, NSERC-CGS, NSERC CGS-MSFSS, NSERC green-SEAM Strategic network, the Mitacs Globalink program, and Hydro-Québec.

CONFLICTS OF INTEREST

The authors state that there are no conflicts to declare.

ACKNOWLEDGMENTS

Authors would like to acknowledge Mr. Pascal Bourseguin for his insight and for fabricating the compression mold used in this work, Dr. Alexandre Romão Costa Nascimento and Mr. Sylvio Savoie for preparing the HVOF coatings, and Mr. Sebasitan Skånvik for assiting with figure aesthetics.

6 REFERENCES

[1] C.H. Simmons, N. Phelps, T.L.D.E. Maguire, Chapter 35 - Bearings and Applied Technology, in: C.H. Simmons, N. Phelps, T.L.D.E.B.T.-M. of E.D. (Fourth E. Maguire (Eds.), Butterworth-Heinemann, Oxford, 2012: pp. 315–330. https://doi.org/https://doi.org/10.1016/B978-0-08-096652-6.00035-8.

[2] T. Kameda, K. Ohkuma, S. Oka, Polytetrafluoroethylene (Ptfe): A resin material for possible use in dental prostheses and devices, Dent. Mater. J. 38 (2019) 136–142. https://doi.org/10.4012/dmj.2018-088.

[3] S.K. Biswas, K. Vijayan, Friction and wear of PTFE — a review, Wear. 158 (1992) 193–211. https://doi.org/https://doi.org/10.1016/0043-1648(92)90039-B.

[4] W.G. Sawyer, K.D. Freudenberg, P. Bhimaraj, L.S. Schadler, A study on the friction and wear behavior of PTFE filled with alumina nanoparticles, Wear. 254 (2003) 573–580. https://doi.org/https://doi.org/10.1016/S0043-1648(03)00252-7.

[5] S. Bahadur, D. Gong, The action of fillers in the modification of the tribological behavior of polymers, Wear. 158 (1992) 41–59. https://doi.org/https://doi.org/10.1016/0043-1648(92)90029-8.

[6] S. Bahadur, D. Tabor, The wear of filled polytetrafluoroethylene, Wear. 98 (1984) 1–13. https://doi.org/https://doi.org/10.1016/0043-1648(84)90213-8.

[7] K. Tanaka, Transfer of semicrystalline polymers sliding against a smooth steel surface, Wear. 75 (1982) 183–199. https://doi.org/https://doi.org/10.1016/0043-1648(82)90147-8.

[8] G. Deli, Z. Bing, X. Qun-Ji, W. Hong-Li, Investigation of adhesion wear of filled polytetrafluoroethylene by ESCA, AES and XRD, Wear. 137 (1990) 25–39. https://doi.org/https://doi.org/10.1016/0043-1648(90)90015-3.

[9] Z.-Z. Zhang, Q.-J. Xue, W.-M. Liu, W.-C. Shen, Friction and wear characteristics of metal sulfides and graphite-filled PTFE composites under dry and oil-lubricated conditions, J. Appl. Polym. Sci. 72 (1999) 751–761. https://doi.org/10.1002/(SICI)1097-4628(19990509)72:6<751::AID-APP3>3.0.CO;2-W.

[10] E.E. Nunez, R. Gheisari, A.A. Polycarpou, Tribology review of blended bulk polymers and their coatings for high-load bearing applications, Tribol. Int. 129 (2019) 92–111. https://doi.org/10.1016/j.triboint.2018.08.002.

[11] J.K. Lancaster, The effect of carbon fibre reinforcement on the friction and wear of polymers, J. Phys. D. Appl. Phys. 1 (1968) 549–559. https://doi.org/10.1088/0022-3727/1/5/303.

[12] J. Bijwe, S. Neje, J. Indumathi, M. Fahim, Friction and Wear Performance Evaluation of Carbon Fibre Reinforced PTFE Composite, J. Reinf. Plast. Compos. 21 (2002) 1221–1240. https://doi.org/10.1177/073168402128987743.

[13] F. Li, F. Yan, L. Yu, W. Liu, The tribological behaviors of copper-coated graphite filled

PTFE composites, Wear. 237 (2000) 33–38. https://doi.org/https://doi.org/10.1016/S0043-1648(99)00303-8.

[14] S.M. Yeo, A.A. Polycarpou, Tribological performance of PTFE- and PEEK-based coatings under oil-less compressor conditions, Wear. 296 (2012) 638–647. https://doi.org/https://doi.org/10.1016/j.wear.2012.07.024.

[15] H. Herman, S. Sampath, R. McCune, Thermal Spray: Current Status and Future Trends, MRS Bull. 25 (2000) 17–25. https://doi.org/10.1557/mrs2000.119.

[16] A. Rempp, A. Killinger, R. Gadow, New Approach to Ceramic/Metal-Polymer Multilayered Coatings for High Performance Dry Sliding Applications, J. Therm. Spray Technol. 21 (2012) 659–667. https://doi.org/10.1007/s11666-011-9731-0.

[17] R. Gadow, D. Scherer, Composite coatings with dry lubrication ability on light metal substrates, Surf. Coatings Technol. 151–152 (2002) 471–477. https://doi.org/https://doi.org/10.1016/S0257-8972(01)01636-X.

[18] M. Yamane, T.A. Stolarski, S. Tobe, Wear and friction mechanism of PTFE reservoirs embedded into thermal sprayed metallic coatings, Wear. 263 (2007) 1364–1374. https://doi.org/https://doi.org/10.1016/j.wear.2006.11.027.

[19] C. Mateus, S. Costil, R. Bolot, C. Coddet, Ceramic/fluoropolymer composite coatings by thermal spraying—a modification of surface properties, Surf. Coatings Technol. 191 (2005) 108–118. https://doi.org/https://doi.org/10.1016/j.surfcoat.2004.04.084.

[20] P.J. Rae, D.M. Dattelbaum, The properties of poly(tetrafluoroethylene) (PTFE) in compression, Polymer (Guildf). 45 (2004) 7615–7625. https://doi.org/https://doi.org/10.1016/j.polymer.2004.08.064.

[21] M. Kokumai, Y. Nakamura, M. Kishine, T. Kitahaba, H. Yukawa, K. Sawada, S.B. Han, T. Shimizu, T. Aoyama, Polytetrafluoroethylene molding powder, (1998).

[22] J.W. Dolan, Polytetrafluoroethylene molding resin and processes, (1998).

[23] Z.H. Zhao, J.N. Chen, Preparation of single-polytetrafluoroethylene composites by the processes of compression molding and free sintering, Compos. Part B Eng. 42 (2011) 1306–1310. https://doi.org/https://doi.org/10.1016/j.compositesb.2011.01.005.

[24] E. Dhanumalayan, G.M. Joshi, Performance properties and applications of polytetrafluoroethylene (PTFE)—a review, Adv. Compos. Hybrid Mater. 1 (2018) 247–268. https://doi.org/10.1007/s42114-018-0023-8.

[25] X.-D. Yuan, X.-J. Yang, A study on friction and wear properties of PTFE coatings under vacuum conditions, Wear. 269 (2010) 291–297. https://doi.org/https://doi.org/10.1016/j.wear.2010.04.014.

[26] Y. Fu, M. Hou, H. Xu, Z. Hou, P. Ming, Z. Shao, B. Yi, Ag–polytetrafluoroethylene composite coating on stainless steel as bipolar plate of proton exchange membrane fuel cell, J. Power Sources. 182 (2008) 580–584.

https://doi.org/https://doi.org/10.1016/j.jpowsour.2008.04.051.

[27] R. Weng, H. Zhang, X. Liu, Spray-coating process in preparing PTFE-PPS composite super-hydrophobic coating, AIP Adv. 4 (2014) 31327. https://doi.org/10.1063/1.4868377.

[28] X. Chen, Y. Gong, X. Suo, J. Huang, Y. Liu, H. Li, Construction of mechanically durable superhydrophobic surfaces by thermal spray deposition and further surface modification, Appl. Surf. Sci. 356 (2015) 639–644. https://doi.org/https://doi.org/10.1016/j.apsusc.2015.08.156.

[29] Y. Kim, C. Chang, A.G. Schrott, Adhesion of metals to spin-coated fluorocarbon polymer films, J. Appl. Phys. 67 (1990) 251–254. https://doi.org/10.1063/1.345298.

[30] S.M. Gateman, K. Page, I. Halimi, A.R.C. Nascimento, S. Savoie, R. Schulz, C. Moreau, I.P. Parkin, J. Mauzeroll, Corrosion of One-Step Superhydrophobic Stainless-Steel Thermal Spray Coatings, ACS Appl. Mater. Interfaces. 12 (2020) 1523–1532. https://doi.org/10.1021/acsami.9b17836.

[31] S.M. Gateman, I. Halimi, A.R. Costa Nascimento, R. Lacasse, R. Schulz, C. Moreau, R. Chromik, J. Mauzeroll, Using macro and micro electrochemical methods to understand the corrosion behavior of stainless steel thermal spray coatings, Npj Mater. Degrad. 3 (2019) 25. https://doi.org/10.1038/s41529-019-0087-0.

[32] P. Samyn, G. Schoukens, Tribological properties of PTFE-filled thermoplastic polyimide at high load, velocity, and temperature, Polym. Compos. 30 (2009) 1631–1646. https://doi.org/10.1002/pc.20737.

[33] L. Mazza, A. Trivella, R. Grassi, G. Malucelli, A comparison of the relative friction and wear responses of PTFE and a PTFE-based composite when tested using three different types of sliding wear machines, Tribol. Int. 90 (2015) 15–21. https://doi.org/https://doi.org/10.1016/j.triboint.2015.04.001.

[34] F. Su, S. Zhang, Tribological properties of polyimide coatings filled with PTFE and surface-modified nano-Si3N4, J. Appl. Polym. Sci. 131 (2014). https://doi.org/doi:10.1002/app.40410.

[35] J.K. Lancaster, Lubrication of carbon fibre-reinforced polymers part I—Water and aqueous solutions, Wear. 20 (1972) 315–333. https://doi.org/10.1016/0043-1648(72)90413-9.

[36] J. Khedkar, I. Negulescu, E.I. Meletis, Sliding wear behavior of PTFE composites, Wear. 252 (2002) 361–369. https://doi.org/https://doi.org/10.1016/S0043-1648(01)00859-6.

[37] S. Zhang, Y. Li, D. Yin, X. Wang, X. Zhao, Y. Shao, S. Yang, Study on synthesis and characterization of novel polyimides derived from 2,6-Bis(3-aminobenzoyl) pyridine, Eur. Polym. J. 41 (2005) 1097–1107. https://doi.org/https://doi.org/10.1016/j.eurpolymj.2004.11.014.

[38] S. A. Alidokht, S. Yue, R.R. Chromik, Effect of WC morphology on dry sliding wear behavior of cold-sprayed Ni-WC composite coatings, Surf. Coatings Technol. 357 (2019)

849–863. https://doi.org/https://doi.org/10.1016/j.surfcoat.2018.10.082.

[39] J.M. Guilemany, S. Dosta, J.R. Miguel, The enhancement of the properties of WC-Co HVOF coatings through the use of nanostructured and microstructured feedstock powders, Surf. Coatings Technol. 201 (2006) 1180–1190. https://doi.org/https://doi.org/10.1016/j.surfcoat.2006.01.041.

[40] N.M. Melendez, V. V Narulkar, G.A. Fisher, A.G. McDonald, Effect of reinforcing particles on the wear rate of low-pressure cold-sprayed WC-based MMC coatings, Wear. 306 (2013) 185–195. https://doi.org/https://doi.org/10.1016/j.wear.2013.08.006.

[41] C.G. McKamey, J.H. DeVan, P.F. Tortorelli, V.K. Sikka, A review of recent developments in Fe3Al-based alloys, J. Mater. Res. 6 (1991) 1779–1805. https://doi.org/DOI: 10.1557/JMR.1991.1779.

[42] S.C. Deevi, V.K. Sikka, C.T. Liu, Processing, properties, and applications of nickel and iron aluminides, Prog. Mater. Sci. 42 (1997) 177–192. https://doi.org/https://doi.org/10.1016/S0079-6425(97)00014-5.

[43] T.C. Totemeier, R.N. Wright, W.D. Swank, Microstructure and stresses in HVOF sprayed iron aluminide coatings, J. Therm. Spray Technol. 11 (2002) 400–408. https://doi.org/10.1361/105996302770348808.

[44] R. Lundy, C. Byrne, J. Bogan, K. Nolan, M.N. Collins, E. Dalton, R. Enright, Exploring the Role of Adsorption and Surface State on the Hydrophobicity of Rare Earth Oxides, ACS Appl. Mater. Interfaces. 9 (2017) 13751–13760. https://doi.org/10.1021/acsami.7b01515.

[45] A.R.C. Nascimento, S. Devaraj, A.P. Francelin, S. Savoie, R. Schulz, C. Moreau, Tailored Porosity for Polymer Infiltration in Stainless Steel Coatings, J. Therm. Spray Technol. 28 (2019) 1173–1184. https://doi.org/10.1007/s11666-019-00884-y.

[46] B. Xu, Z. Zhu, S. Ma, W. Zhang, W. Liu, Sliding wear behavior of Fe–Al and Fe–Al/WC coatings prepared by high velocity arc spraying, Wear. 257 (2004) 1089–1095. https://doi.org/https://doi.org/10.1016/j.wear.2004.05.012.

[47] M. Amiriyan, C. Blais, S. Savoie, R. Schulz, M. Gariépy, H. Alamdari, Tribo-Mechanical Properties of HVOF Deposited Fe3Al Coatings Reinforced with TiB2 Particles for Wear-Resistant Applications, Mater. . 9 (2016). https://doi.org/10.3390/ma9020117.

[48] M. Amiriyan, C. Blais, S. Savoie, R. Schulz, M. Gariépy, D.H. Alamdari, Mechanical Behavior and Sliding Wear Studies on Iron Aluminide Coatings Reinforced with Titanium Carbide, Met. . 7 (2017). https://doi.org/10.3390/met7050177.

[49] C. Demian, H. Liao, R. Lachat, S. Costil, Investigation of surface properties and mechanical and tribological behaviors of polyimide based composite coatings, Surf. Coatings Technol. 235 (2013) 603–610. https://doi.org/https://doi.org/10.1016/j.surfcoat.2013.08.032.

[50] W. Jiang, G. Nadeau, K. Zaghib, K. Kinoshita, Thermal analysis of the oxidation of

natural graphite — effect of particle size, Thermochim. Acta. 351 (2000) 85–93. https://doi.org/https://doi.org/10.1016/S0040-6031(00)00416-0.

[51] E. Basavaraj, B. Ramaraj, Siddaramaiah, Investigations on the influence of polytetrafluoroethylene powder as a filler on physico-mechanical and wear characteristics of nylon 66/graphite composites, High Perform. Polym. 24 (2012) 616–624. https://doi.org/10.1177/0954008312446765.

[52] B. Bernard, A. Quet, L. Bianchi, V. Schick, A. Joulia, A. Malié, B. Rémy, Effect of Suspension Plasma-Sprayed YSZ Columnar Microstructure and Bond Coat Surface Preparation on Thermal Barrier Coating Properties, J. Therm. Spray Technol. 26 (2017) 1025–1037. https://doi.org/10.1007/s11666-017-0584-z.

[53] F. Caio, C. Moreau, Influence of Substrate Shape and Roughness on Coating Microstructure in Suspension Plasma Spray, Coatings . 9 (2019). https://doi.org/10.3390/coatings9110746.

[54] K. Maghsoudi, G. Momen, R. Jafari, M. Farzaneh, Direct replication of micro-nanostructures in the fabrication of superhydrophobic silicone rubber surfaces by compression molding, Appl. Surf. Sci. 458 (2018) 619–628. https://doi.org/https://doi.org/10.1016/j.apsusc.2018.07.099.

[55] G. Bhat, A review of: "Injection and Compression Molding Fundamentals" Edited by Avraam I. Isayev, Mater. Manuf. Process. 9 (1994) 1005–1006. https://doi.org/10.1080/10426919408934967.

[56] L. Ding, D. Axinte, P. Butler-Smith, A. Abdelhafeez Hassan, Study on the characterisation of the PTFE transfer film and the dimensional designing of surface texturing in a dry-lubricated bearing system, Wear. 448–449 (2020) 203238. https://doi.org/https://doi.org/10.1016/j.wear.2020.203238.

[57] Y. Sujuan, Z. Xingrong, Tribological Properties of PTFE and PTFE Composites at Different Temperatures, Tribol. Trans. 57 (2014) 382–386. https://doi.org/10.1080/10402004.2013.812759.

[58] Y. Wang, F. Yan, Tribological properties of transfer films of PTFE-based composites, Wear. 261 (2006) 1359–1366. https://doi.org/https://doi.org/10.1016/j.wear.2006.03.050.

[59] Y. Zhang, D. Chern, R. Schulz, J. Mauzeroll, R.R. Chromik, Manufacturing and Tribological Behavior of Self-Lubricating Duplex Composites: Graphite-Reinforced Polymer Composites and Polymer-Infiltrated Metal Networks, J. Mater. Eng. Perform. 30 (2021) 103–115. https://doi.org/10.1007/s11665-020-05329-0.

[60] P.S. Ho, P.O. Hahn, J.W. Bartha, G.W. Rubloff, F.K. LeGoues, B.D. Silverman, Chemical bonding and reaction at metal/polymer interfaces, J. Vac. Sci. Technol. A Vacuum, Surfaces Film. 3 (1985) 739–745. https://doi.org/10.1116/1.573298.

[61] D.L. Allara, F.M. Fowkes, J. Noolandi, G.W. Rubloff, M. V Tirrell, Bonding and adhesion of polymer interfaces, Mater. Sci. Eng. 83 (1986) 213–226.

https://doi.org/10.1016/0025-5416(86)90339-3.

[62] L. Atanasoska, S.G. Anderson, H.M. Meyer, Z. Lin, J.H. Weaver, Aluminum/polyimide interface formation: An x-ray photoelectron spectroscopy study of selective chemical bonding, J. Vac. Sci. Technol. A. 5 (1987) 3325–3333. https://doi.org/10.1116/1.574191.

[63] L.P. Buchwalter, Adhesion of polyimides to metal and ceramic surfaces: an overview, J. Adhes. Sci. Technol. 4 (1990) 697–721. https://doi.org/10.1163/156856190X00612.

[64] S.W. Lee, J.W. Hong, M.Y. Wye, J.H. Kim, H.J. Kang, Y.S. Lee, Surface modification and adhesion improvement of PTFE film by ion beam irradiation, Nucl. Instruments Methods Phys. Res. Sect. B Beam Interact. with Mater. Atoms. 219–220 (2004) 963–967. https://doi.org/https://doi.org/10.1016/j.nimb.2004.01.197.

[65] R.R. Rye, J.A. Knapp, K. -M. Chi, M.J. Hampden-Smith, T.T. Kodas, Formation of copper patterns on poly(tetrafluoroethylene) via radiation controlled chemical etching and chemical-vapor deposition, J. Appl. Phys. 72 (1992) 5941–5947. https://doi.org/10.1063/1.351902.

[66] P.A. Ingemarsson, M.P. Keane, U. Gelius, Chemical modifications at Teflon interfaces induced by MeV ion beams, J. Appl. Phys. 66 (1989) 3548–3553. https://doi.org/10.1063/1.344083.

[67] N. Inagaki, S. Tasaka, Y.W. Park, Effects of the surface modification by remote hydrogen plasma on adhesion in the electroless copper / tetrafluoroethylene - hexafluoropropylene copolymer (FEP) system, J. Adhes. Sci. Technol. 12 (1998) 1105–1119. https://doi.org/10.1163/156856198X00768.

Table I: Elemental analysis of the Fe_3Al HVOF coatings' surface via EDX. Values are 9 spots that were averaged at 95% confidence intervals.

Element	Fe	Al	C	O	Cr	Si
wt%	69.3 ± 8.6	13.2 ± 2.8	7.9 ± 2.1	7.5 ± 6.4	1.9 ± 0.3	0.3 ± 0.1

Table II: Comparison of tribological properties including COF and wear rates of some coatings and materials reported in literature and coatings produced in this work at 95% confidence intervals. * Represents results from the presented work.

Ref	Coating	COF	Wear Rate (10^{-4} mm^3/Nm)	Fabrication Process	Set Up	Counter Material, Load Applied, Sliding Velocity, RH
[33]	PTFE	0.21 ± 0.02	23.1 ± 2.5	Compression molding	Pin-on-disk	10 N, anodized Al, 2.3 m/s, 50 %
[34]	PI	0.35	2.7	Air spray	Ball-on-disk	GCr15 Steel, 4.0 N, 0.33 m/s, N/A
[34]	20% PTFE/ 80% PI	0.15	1.3	Air spray	Ball-on-disk	GCr15 Steel, 4.0 N, 0.33 m/s, N/A
[33]	85% PTFE/ 15% PI	0.13 ± 0.03	1.1 ± 0.2	Compression molding	Pin-on-disk	10 N, anodized Al, 2.3 m/s, 50 %
*	80% PTFE/ 20% PI	0.10 ± 0.02	0.4 ± 0.1	Compression molding	Ball-on-flat	AISI stainless steel 440C, 10.7 N, 0.01 m/s, 30-35%
*	75% PTFE/ 20% PI/ 5% Graphite	0.10 ± 0.01	0.5 ± 0.4	Compression molding	Ball-on-flat	AISI stainless steel 440C, 10.7 N, 0.01 m/s, 30-35%

Table III: Elemental composition of points analyzed in Figure 7 as wt%.

Point	C	F	O	Cr
Red	32.7	67.3	--	--
Blue	18.9	75.0	--	6.1
Green	70.5	4.3	25.2	--
Violet	23.4	76.6	--	--

Table IV: Elemental composition of points analyzed in Figure 8 as wt%.

Point	C	N	O	F	Fe	Pt	Cr
Red	33.7	--	1.9	62.9	--	1.6	--
Blue	63.9	6.10	15.3	0.1	0.1	13.8	0.8
Green	40.1	--	--	57.5	--	2.4	--
Violet	98.3	--	1.5	--	--	0.3	--

Figure 1: Schematic of the compression press mold fabricated for the present work.

Figure 2: (A) SEM image of the as sprayed Fe_3Al HVOF coating's surface and (B) A magnified image showing the material's surface roughness.

Figure 3: Thermal gravimetric thermograms of PTFE/PI and PTFE/PI/Graphite powders performed under air and ramped at a rate of 20 °C/min.

Figure 4: Electron microscopy images of the layered composite coating's cross sections without (A) and with (B) the addition of graphite. Magnified images of the interfaces between the thermal spray and polymer coatings are shown in (i) without and (ii) with graphite, showing corresponding EDX mappings of Fe, F, and C.

Figure 5: (A) SEM image of the composite polymeric surface and (B) corresponding average surface roughness measurements at a 95% confidence interval.

Figure 6: The coefficient of friction as a function of cycle number of the (A) PTFE/PI and (B) PTFE/PI/graphite coatings under 10.7 N load and a wear track of 6 mm.

Figure 7: Backscatter electron microscopy image of the counter spheres after wear measurements on the thick PTFE/PI coatings (A) and PTFE/PI coatings with 5 wt% graphite (B). White arrows indicate sliding directions.

Figure 8: Back-scattered electron microscopy images and EDS chemical point analysis of wear tracks resulting from wear measurements on the PTFE/PI coatings (A and B) and PTFE/PI coatings with 5 wt% graphite (C and D). All images show the enrichment of PI inside the wear track, as shown by the dark regions and pointed out with black arrows. The sliding direction is shown by the white double arrows.

Figure 9: X-ray photoelectron spectroscopy spectra for the C 1s region obtained over crossed sections of PI/PTFE and PI/PTFE/graphite coatings carried out over the HVOF coatings, the polymeric films, and at the interface.

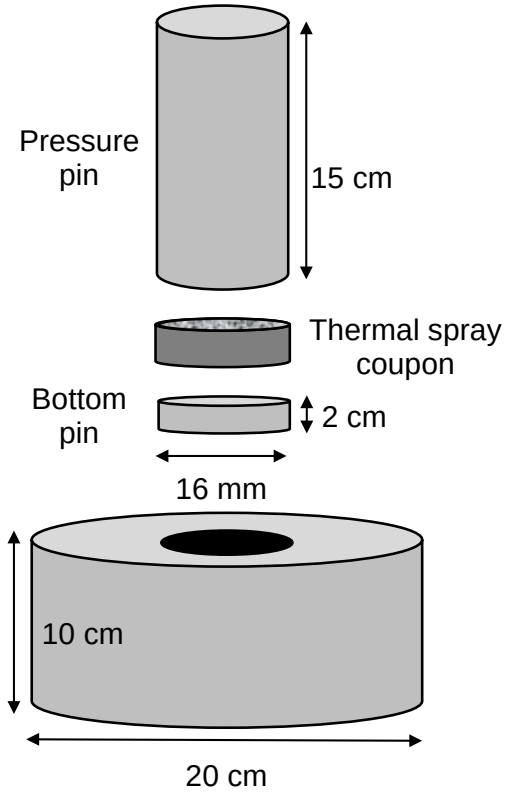

Figure 1.

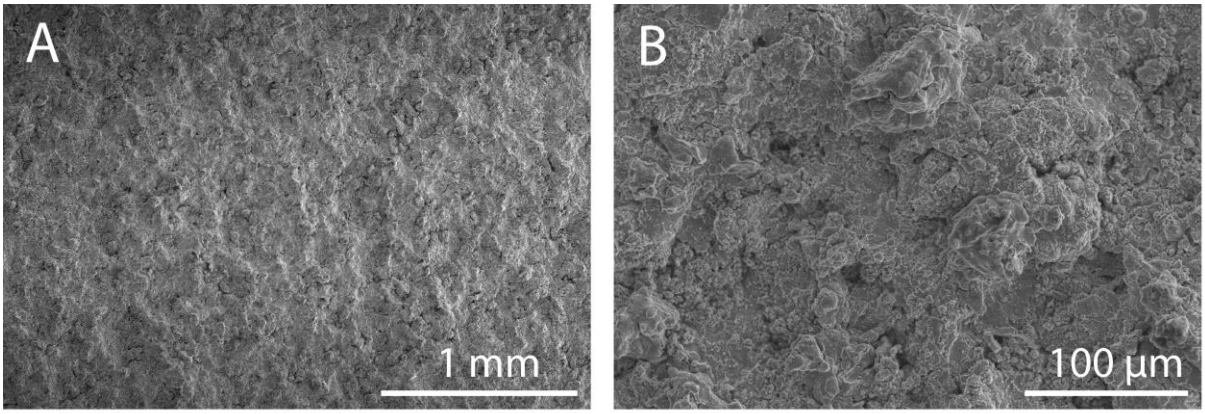

Figure 2.

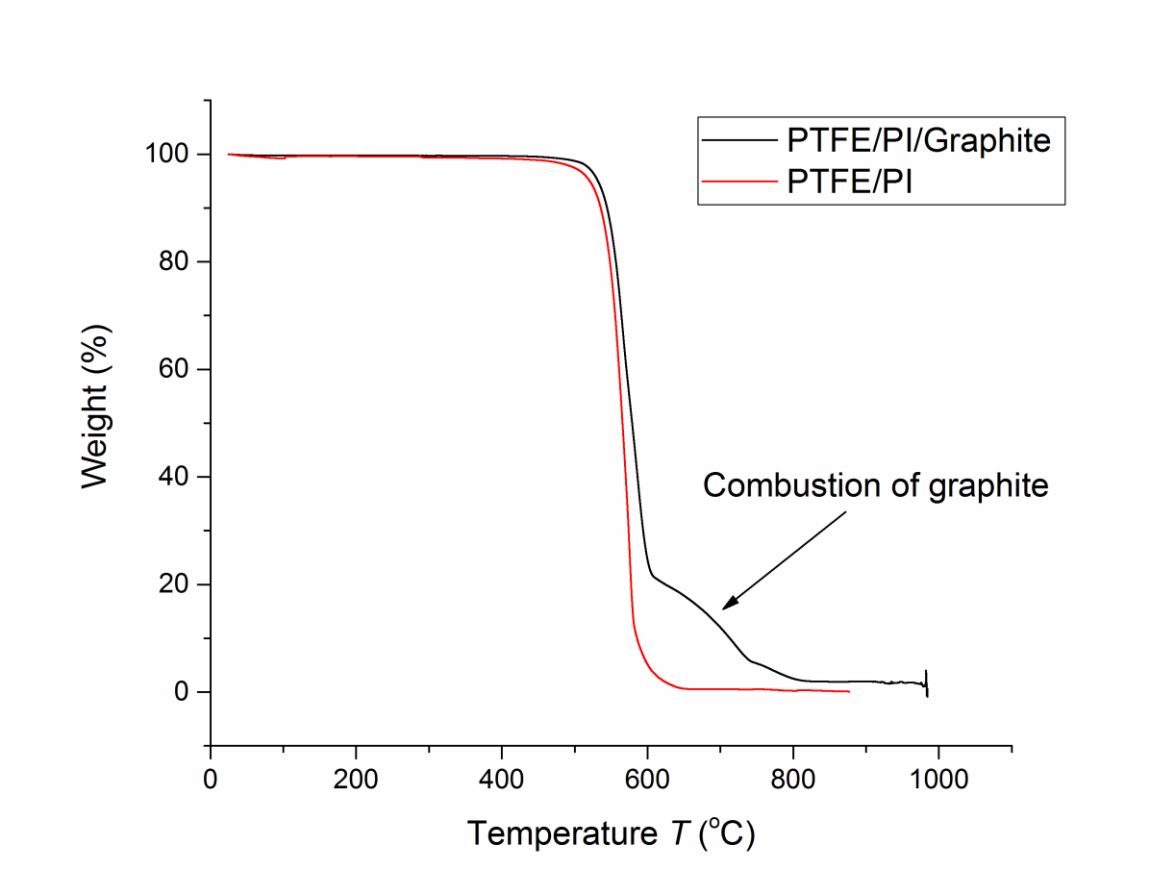
PTFE/PI/Graphite
PTFE/PI
Combustion of graphite
Weight (%)
Temperature T (°C)
100
80
60
40
20
0
0
200
400
600
800
1000

Figure 3.

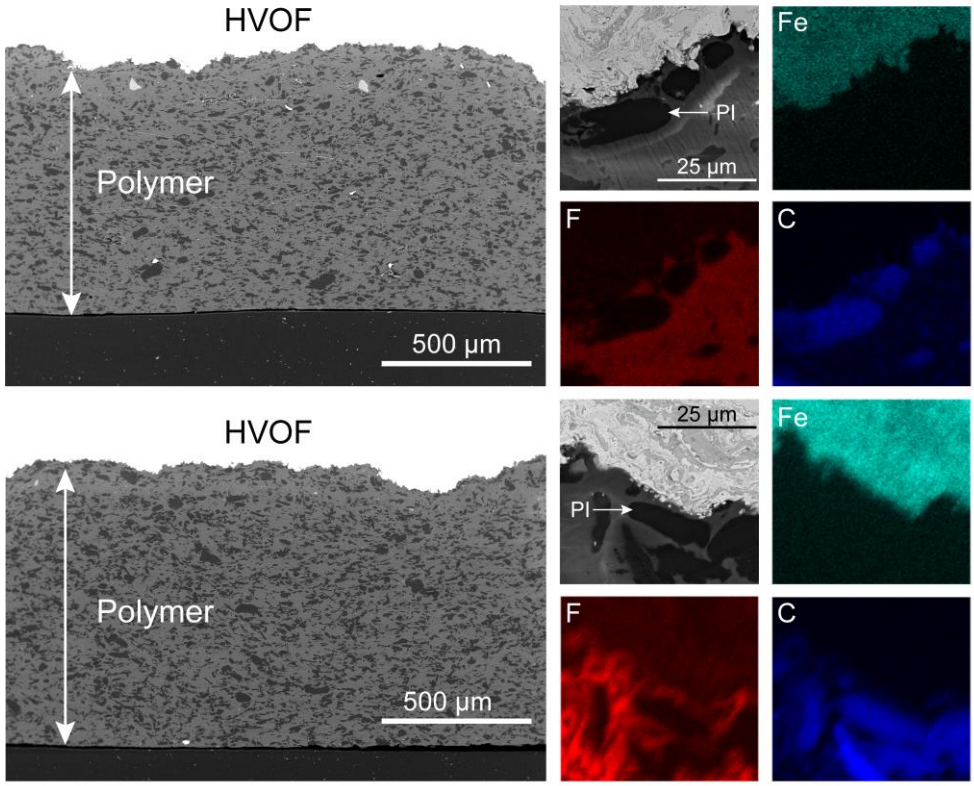
HVOF
Polymer
500 µm
Pl
25 µm
Fe
F
C
HVOF
Polymer
500 µm
25 µm
Pl
Fe
F
C

Figure 4.